

## RESEARCH ARTICLE

# Toll-like receptor 2 (TLR2) engages endoplasmic reticulum stress sensor IRE1 $\alpha$ to regulate retinal innate responses in *Staphylococcus aureus* endophthalmitis

Ajay Kumar<sup>1</sup> | Pawan Kumar Singh<sup>1</sup> | Kezhong Zhang<sup>2,3</sup> | Ashok Kumar<sup>1,3</sup>

<sup>1</sup>Department of Ophthalmology, Visual and Anatomical Sciences/Kresge Eye Institute, Wayne State University School of Medicine, Detroit, MI, USA

<sup>2</sup>Center for Molecular Medicine and Genetics, Wayne State University School of Medicine, Detroit, MI, USA

<sup>3</sup>Department of Biochemistry, Microbiology, and Immunology, Wayne State University School of Medicine, Detroit, MI, USA

**Correspondence**

Ashok Kumar, Department of Ophthalmology, Visual and Anatomical Sciences, Wayne State University School of Medicine, 4717 St. Antoine, Detroit, MI 48201, USA.  
Email: akuma@med.wayne.edu

**Present address**

Ajay Kumar, Department of Microbiology and Immunology, University of Michigan Medical School, Ann Arbor, MI, USA

**Funding information**

NIH/NEI, Grant/Award Number: R01EY026964 and R01EY027381; NIH/NIAID, Grant/Award Number: R21AI140033 and R21AI135583; NIH, Grant/Award Number: DK090313

**Abstract**

Endoplasmic reticulum (ER) stress response has been implicated in a variety of pathophysiological conditions, including infectious and inflammatory diseases. However, its contribution in ocular bacterial infections, such as endophthalmitis, which often cause blindness is not known. Here, using a mouse model of *Staphylococcus* (*S.*) *aureus* endophthalmitis, our study demonstrates the induction of inositol-requiring enzyme 1 $\alpha$  (IRE1 $\alpha$ ) and splicing of X-box binding protein-1 (*Xbp1*) branch of the ER-stress pathway, but not the other classical ER stress sensors. Interestingly, *S aureus*-induced ER stress response was found to be dependent on Toll-like receptor 2 (TLR2), as evident by reduced expression of IRE1 $\alpha$  and *Xbp1* mRNA splicing in TLR2 knockout mouse retina. Pharmacological inhibition of IRE1 $\alpha$  using 4 $\mu$ 8C or experiments utilizing IRE1 $\alpha$ <sup>-/-</sup> macrophages revealed that IRE1 $\alpha$  positively regulates *S aureus*-induced inflammatory responses. Moreover, IRE1 $\alpha$  inhibition attenuated *S aureus*-triggered NF- $\kappa$ B, p38, and ERK pathways activation and cells treated with these pathway-specific inhibitors reduced *Xbp1* splicing, suggesting a positive feedback inhibition. In vivo, inhibition of IRE1 $\alpha$  diminished the intraocular inflammation and reduced PMN infiltration in mouse eyes, but, increased the bacterial burden and caused more retinal tissue damage. These results revealed a critical role of the IRE1 $\alpha$ /XBP1 pathway as a regulator of TLR2-mediated protective innate immune responses in *S aureus*-induced endophthalmitis.

**KEY WORDS**

endophthalmitis, endoplasmic reticulum (ER) stress, inflammation, microglia, reactive oxygen species (ROS), retina, *S aureus*, toll-like receptor 2 (TLR2)

**Abbreviations:** ARVO, Association for Research in Vision and Ophthalmology; ATF6, activating transcription factor 6; BMDM, bone marrow-derived macrophages; BSA, bovine serum albumin; CXCL1, chemokine (C-X-C motif) ligand 1; CXCL2, chemokine (C-X-C motif) ligand 2; DLAR, division of laboratory animal resources; DMEM, Dulbecco's Modified Eagle Medium; EDTA, ethylenediaminetetraacetic acid; ELISA, enzyme-linked immunosorbent assay; ER, endoplasmic reticulum; FBS, fetal bovine serum; H&E, hematoxylin and eosin; HRP, Horseradish peroxidase; IL-1 $\beta$ , interleukin-1beta; IL6, interleukin-6; IRE1 $\alpha$ , inositol-requiring enzyme 1 $\alpha$ ; KC, keratinocyte chemoattractant; LPS, lipopolysaccharides; LTA, lipoteichoic acid; M-CSF, macrophage colony-stimulating factor; MIP2, macrophage inflammatory protein 2; mM, millimolar; MOI, multiplicity of infection; NF- $\kappa$ B, nuclear factor kappa-light-chain-enhancer of activated B cells; PCR, polymerase chain reaction; PERK, protein kinase RNA-like ER kinase; PGN, peptidoglycan; PMN, polymorphonuclear cells; RNA, ribonucleic acid; ROS, reactive oxygen species; SA, *S aureus*; TLR2, toll-like receptor 2; TNF $\alpha$ , tumor necrosis factor-alpha; TUNEL, terminal deoxynucleotidyl transferase dUTP nick end labeling; UPR, unfolded protein response; WT, wild type; XBP1, X-box binding protein-1.

## 1 | INTRODUCTION

*Staphylococcus (S) aureus* has long been recognized as an important bacterial pathogen causing various human diseases including infection of the bloodstream, skin, bone, and joints as well as pneumonia.<sup>1-3</sup> Aside from the aforementioned manifestations, *S aureus* remains the leading cause of ocular diseases, such as bacterial endophthalmitis, which often results in poor prognosis even after treatment.<sup>4</sup> Mostly, ocular trauma or surgical procedures predispose the eye to develop bacterial endophthalmitis.<sup>5,6</sup> Visual prognosis mainly depends on the virulence properties of the causative organism, visual ingenuity, and the efficacy of the antimicrobial treatment regime.<sup>7</sup> Eye being an immunoprivileged organ, the retina is highly susceptible to host-induced inflammatory damage along with the injury caused by pathogens virulence factors. Previously, we have shown that retinal cells including Müller glia, microglia, and photoreceptors cells mount a massive innate immune response against *S aureus* infection that could contribute to the retinal damage in addition to providing protection against pathogen.<sup>8-10</sup> Studies from both our laboratory and others have sought to elucidate the role of Toll-like receptors (TLRs) in the initiation of innate defense mechanisms in bacterial endophthalmitis.<sup>4,8,11-15</sup> Of particular interest is TLR2, which has been found to orchestrate protective retinal innate immune responses in *Staphylococcal* endophthalmitis via modulating intraocular inflammation, and induction of antimicrobial peptides.<sup>4,8,11,15</sup>

Endoplasmic reticulum (ER) is an intricate cellular organelle present in eukaryotic cells. The ER is a major site for protein synthesis and maturation and is involved in the processing of secretory and membrane proteins.<sup>16,17</sup> A wide variety of cellular conditions, including glucose deprivation, disruption of calcium homeostasis, and both viral and bacterial infections, have been implicated as the causative agent behind the influx of unfolded or misfolded peptides which results in an ER stress response. To deal with this stress, the ER has evolved a set of signal transduction pathways that are collectively termed as unfolded protein response (UPR). For sensing ER stress, three major transmembrane transducers have been identified: Protein kinase RNA-like ER kinase (PERK), Inositol requiring enzyme (IRE1 $\alpha$ ), and activating transcription factor 6 (ATF6). Compared to other stress sensors, IRE1 $\alpha$  is the most conserved signaling branch. IRE1 $\alpha$  activation induces unconventional splicing of a 26-nucleotide intron from the RNA encoding X-box binding protein 1 (XBP1) to convert into mature XBP1s which then acts as a transcription factor.<sup>18</sup> The IRE1 $\alpha$ -XBP1 branch is evolutionary conserved from yeast to human and is essential for mammalian developmental processes.<sup>19</sup> The cytoplasmic portion of IRE1 $\alpha$  has both kinase and endonuclease activities, whereas the luminal domain can detect unfolded proteins. The IRE1 $\alpha$ -induced XBP1s then activates the downstream

genes, including the ER chaperones ERDj4, GRP78 (BiP), and PDI which are known to play a central role in restoring cellular ER homeostasis and promoting cell survival.<sup>20,21</sup> If ER stress is sustained for too long, it can result in persistent inflammation and eventual cell death.<sup>22</sup>

Transcriptional induction of the *Xbp1* mRNA precursor after TLR stimulations in human macrophage, as well as mouse lung tissues during *Mycobacterium* and *Klebsiella* infection, have been reported.<sup>23,24</sup> ER stress response has been shown to either support or hamper disease progression by regulating inflammatory host defense pathways depending on the cell types, disease model, and the ER stressor.<sup>25</sup> It has been shown that some intracellular pathogens utilize ER stress signaling as a protective mechanism for their intracellular growth and UPR induction is beneficial to the infection.<sup>26</sup> Previously, TLR2 and TLR4 ligands-mediated activation of ER stress response have been shown, which demonstrates a novel mechanism of IRE1 activation independent of protein misfolding in the ER lumen.<sup>27,28</sup> Nevertheless, the role of ER stress response in ocular infections, especially in bacterial endophthalmitis remains largely unexplored. Recently, we performed a transcriptomic analysis in *S aureus* infected mouse retina<sup>29</sup> and discovered dysregulation of genes modulating ER stress response including *Xbp1* and *Bip*. Therefore, we initiated this study to investigate the role of ER stress in the bacterial ocular infection.

In the current study, we show that *S aureus* infection in the eye specifically induces the IRE1 $\alpha$ /XBP1 axis of ER stress. Notably, we found that IRE1 $\alpha$  is essential for the induction of TLR2-mediated innate inflammatory responses and that the abrogation of this pathway is detrimental. In accordance, IRE1 $\alpha$  inhibition resulted in increased bacterial burden and retinal tissue damage in the eye. These results suggest that IRE1 $\alpha$ /XBP1 signaling is a protective host response in ocular infections.

## 2 | MATERIALS AND METHODS

### 2.1 | Animals

C57BL/6 [wild type (WT)] mice (both male and female, 6-8 weeks of age) were purchased from the Jackson Laboratory (Bar Harbor, ME). TLR2<sup>-/-</sup> breeders were purchased from Jackson Laboratory, bred in-house, and maintained in a pathogen-free, restricted-access Division of Laboratory Animal Resources (DLAR) facility at Kresge Eye Institute. IRE1 $\alpha$ <sup>fllox/fllox</sup> and myeloid cell-specific IRE1 $\alpha$ <sup>-/-</sup> mice<sup>28</sup> were provided by Dr Kezhong Zhang (Center for Molecular Medicine and Genetics, Wayne State University). All animals were maintained on a 12 hours light 12 hours dark cycle at 22°C temperature and provided free access to the tap water and LabDiet rodent chow (PicoLab; LabDiet,

St. Louis, MO). All the procedures were conducted in compliance with the Association for Research in Vision and Ophthalmology (ARVO) statement for the Use of Animals in Ophthalmic and Vision Research and were approved by the Institutional Animal Care and Use Committee (IACUC) of Wayne State University.

## 2.2 | Cell culture

An immortalized mouse microglia (BV2) cell line was maintained in low-glucose Dulbecco's Modified Eagle Medium (DMEM) supplemented with 5% FBS and a penicillin-streptomycin cocktail (Invitrogen, Carlsbad, CA) in a humidified 5% CO<sub>2</sub> incubator at 37°C. Before treatment, cells were cultured in antibiotic-free and serum-free DMEM for 18 hours (growth factor starvation). Cells were either stimulated with TLR agonist Pam3CysSK4 (10 µg/mL) or infected with *S aureus* RN6390 multiplicity of infection (MOI) 10:1 for 8 hours.

## 2.3 | Induction of *S aureus* endophthalmitis

Endophthalmitis was induced in mice as described previously.<sup>4,10</sup> Briefly, mice were anesthetized by intraperitoneal injection of ketamine/xylazine (ketamine, 100-125 mg/kg; xylazine, 10-12.5 mg/kg). Under an ophthalmoscope, mice left eyes were injected intravitreally with *S aureus* strain RN6390 (500 0CFU/eye) using a 34G needle attached to a 10 µL syringe (WPI). Contralateral eyes injected with sterile PBS served as control. At the desired time points postinfection; enucleated eyes or neural retina were subjected to bacterial growth determination, inflammatory cytokines/chemokines assays, western blotting, and histology as described in the following sections.

## 2.4 | Isolation of bone marrow-derived macrophage (BMDM)

Bone marrow-derived macrophages (BMDM) were isolated as described previously.<sup>30,31</sup> Briefly, bone marrow cells from *IRE1α<sup>fllox/fllox</sup>* and myeloid cell-specific *IRE1α* KO mice were flushed from femurs and tibias using RPMI media containing 10% FBS and 0.2 mM EDTA. RBCs were lysed by adding a hypotonic solution of 0.2% NaCl for 20 s, followed by the addition of 1.6% NaCl. Bone marrow cells were pelleted by centrifugation at 400g for 5 minutes followed by a wash with RPMI media. Cells were resuspended, counted, and cultured in RPMI media supplemented with 10% FBS, 100 U/mL penicillin, 100 mg/mL streptomycin, and 10 ng/mL M-CSF at 37°C in 5% CO<sub>2</sub> for macrophage differentiation. Six days

post-differentiation  $\sim 1 \times 10^6$  BMDM/mL were seeded in 6-well tissue-culture plates for in vitro experiments.

## 2.5 | RNA extraction and polymerase chain reaction (PCR)

Total RNA was extracted from both mouse neural retina and BV2 cells using TRIzol per manufacturer's instructions (Invitrogen, Carlsbad, CA, USA). One microgram of total RNA was reversed transcribed using Maxima first-strand cDNA synthesis kit per manufacturer's instructions (Thermo Scientific, Rockford, IL, USA). cDNA was amplified for a gene of interest by PCR using mouse-specific primers. PCR products along with housekeeping internal control GAPDH, were subjected to electrophoresis on 2.5% or 1.2% agarose gel according to the size of the PCR amplicons. For XBP1 splicing detection, both, unspliced and spliced forms of XBP1 mRNA species were resolved using high-percentage (2.5%) agarose gel electrophoresis which is often used to detect *IRE1α* endonuclease activity. Images of ethidium bromide-stained gels were captured using a digital camera (EDAS 290 system, Eastman Kodak, Rochester, NY).

## 2.6 | Enzyme-linked immunosorbent assay (ELISA)

ELISA was performed to quantify the levels of cytokines/chemokines in mice ocular tissue as well as the cells conditioned media. Briefly, mouse eyes were enucleated and homogenized in sterile PBS by stainless steel beads using Tissue lyser (Qiagen, Valencia, CA) followed by centrifugation at 15 000g for 15 minutes. Total protein was estimated using the Micro BCA protein estimation kit (Thermo Scientific, Rockford, IL, USA) per manufacturer's instructions. ELISA was performed for tumor necrosis factor-alpha (TNF-α), interleukin-1beta (IL-1β), interleukin-6 (IL-6) (BD biosciences, San Diego, CA, USA), macrophage inflammatory protein 2 (MIP2/CXCL2), and CXCL1/KC (R&D systems, Minneapolis, MN, USA) per manufacturer's instructions.

## 2.7 | Histology and terminal deoxynucleotidyl transferase dUTP nick end labeling (TUNEL) assay

Mice eyes were enucleated at desired time points for histopathological examination and fixed in 10% formalin. Embedding, sectioning, and hematoxylin and eosin (H&E) staining were performed by Excalibur Pathology Inc (Oklahoma City, OK, USA). All retinal H&E sections were observed with a light microscope (400× magnification). For

TUNEL staining, the eyes were fixed in Tissue-Tek OCT (Sakura, Torrance, CA, USA) and 6-8  $\mu\text{m}$  thick sagittal sections were collected from each eye and mounted onto microscope slides. Retinal sections were used for the TUNEL staining using ApopTag Fluorescein In situ Apoptosis Detection Kit according to the manufacturer's instruction (Millipore, Billerica, MA, USA).

## 2.8 | Polymorphonuclear cells (PMNs) infiltration

To determine the PMNs infiltration in mice retina, flow cytometry was used as described previously.<sup>32</sup> Briefly, following euthanasia, retinas were isolated and digested with Accumax (Millipore, MA, USA) for 10 minutes at 37°C. A single-cell suspension was prepared by triturating the retina using a 23-G needle/syringe and filtered through a 40  $\mu\text{m}$  cell strainer (BD Falcon, San Jose, CA, USA). To reduce the nonspecific binding of antibodies, cells were incubated with Fc Block (BD Biosciences) for 30 minutes. After washing with 0.5% BSA, cell suspensions were incubated with conjugated monoclonal antibodies CD45-PECy5, Ly6G-FITC, and respective isotype controls (BD Biosciences) in dark for 30 minutes. After washing, cells were acquired and analyzed using the Accuri C6 flow cytometer and software (BD Biosciences, San Jose, CA, USA), respectively.

## 2.9 | Immunoblotting

For immunoblotting, cells were lysed using radioimmunoprecipitation (RIPA) lysis buffer containing a protease and phosphatase inhibitor cocktail (Thermo Scientific, Rockford, IL, USA). Mice neural retinas were lysed by sonication in PBS containing a protease and phosphatase inhibitor cocktail. Total protein concentration was determined, and 30-40  $\mu\text{g}$  protein was used for blotting. Denatured proteins were resolved on a 12% SDS-polyacrylamide gel and transferred onto a nitrocellulose membrane (0.44  $\mu\text{m}$ ) (Bio-Rad Laboratories). Following blocking, the blots were incubated with anti-phospho (Ser-51)-IRE1 $\alpha$ , anti-total IRE1 $\alpha$  (1:1000) (Cell signaling Technology, Boston, MA), and anti- $\beta$ -actin (1:5000) (Sigma-Aldrich, St. Louis, MO) antibodies overnight at 4°C. Following washing, blots were incubated with goat anti-rabbit/ mice IgG-HRP conjugate (BioRad, Hercules, CA). Protein bands were developed using SuperSignal West Femto Chemiluminescent Substrate and visualized using iBright FL1500 Imaging Systems (Thermo Fisher Scientific, Rockford, IL).  $\beta$ -actin was used as a control for protein loading. Quantification of the intensity of bands was performed using ImageJ software (Rasband, WS, ImageJ, US National

Institutes of Health, Bethesda, Maryland, <http://rsb.info.nih.gov/ij/>, 1997-2009).

## 2.10 | Immunostaining

Immunostaining was performed as described earlier.<sup>33,34</sup> Briefly, cells were cultured on four well glass chamber slides (Fisher Scientific, Rochester, NY) and pre-treated with 4 $\mu\text{M}$  IRE1 $\alpha$  inhibitor 1 hour before *S aureus* challenge. Following stimulation, cells were washed three times with PBS and fixed in 4% paraformaldehyde for 15 minutes. Cells were permeabilized with an ethanol: acetic acid mixture (2:1) at -20°C for 10 minutes and washed. The fixed cells were blocked in 1% (w/v) BSA for 1 hour at room temperature followed by incubation with primary antibodies (1:100 dilution) overnight at 4°C. Cells were washed with PBS and incubated with specific fluorescein isothiocyanate (FITC)-conjugated secondary antibodies (1:200 dilutions) for 1 hour at room temperature. Following incubation cells were washed with PBS and mounted in Vectashield anti-fade mounting medium with DAPI (Vector Laboratories). Slides were visualized using an Eclipse 90i fluorescence microscope (Nikon, Melville, NY).

## 2.11 | Statistical analysis

Statistical analysis was performed using GraphPad Prism V8 (GraphPad Software, La Jolla, CA). All data has been expressed as means  $\pm$  SD unless indicated otherwise. Unpaired student *t* test or One-way ANOVA was used for comparisons followed by Dunnett's' post hoc test wherever applicable. A *P* value of <0.05 was considered statistically significant. All experiments were performed at least three times unless indicated otherwise.

# 3 | RESULTS

## 3.1 | ER stress is induced during *S aureus* endophthalmitis

Bacterial infections have been shown to trigger an UPR<sup>35,36</sup> resulting in the activation of the ER-transmembrane protein IRE1 $\alpha$ . Although multiple targets for the IRE1 $\alpha$  endonuclease have been identified, the splicing of *Xbp1* mRNA is the main under infectious and inflammatory conditions.<sup>37</sup> To assess whether IRE1 $\alpha$ -XBP1 or other ER stress sensors are induced in bacterial endophthalmitis, we analyzed transcriptomic data that had been previously published.<sup>29</sup> Indeed, our data showed a time-dependent induction of *XBP1* (Figure 1A, upper panel) and *BiP* (Figure 1A, lower panel) mRNA transcripts upon *S*

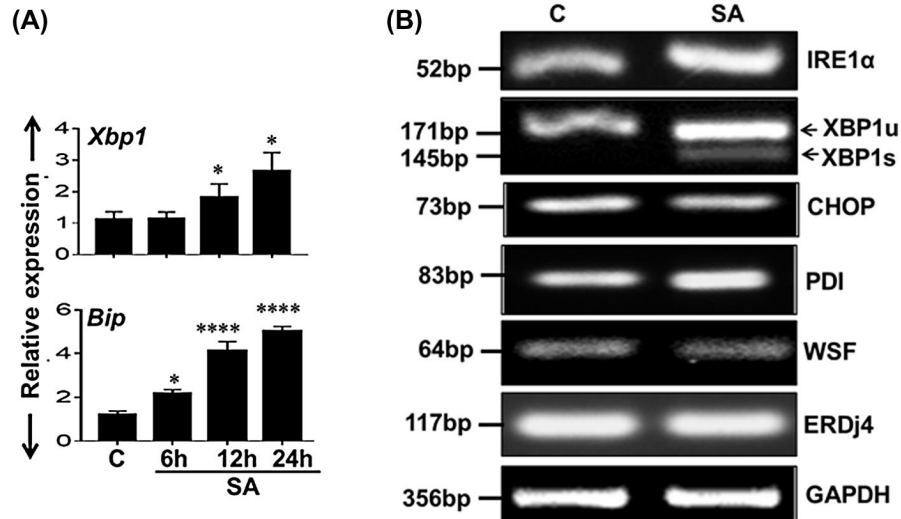


**FIGURE 1** *S aureus* infection induces ER stress in the mouse retina. C57BL/6 mouse (n = 6) eyes were intravitreally injected with PBS (control, C) or 5000 CFU of *S aureus* (SA), strain RN6390. At indicated time point postinfection, eyes were enucleated, and retinal tissue was subjected to temporal transcriptomic analysis using microarray (reported previously).<sup>29</sup> The microarray data showed induced expression of *Xbp1* and *Bip* genes. The data are expressed as relative fold change by normalizing the expression of genes with respect to control (A). In another set of experiments, RNA was extracted from SA-infected retinal tissue at 24 hours and subjected to RT-PCR to detect mRNA expression of indicated ER stress markers (B). Results are representative of at least two independent (n = 6 each) experiments. Statistical analysis was performed using one-way ANOVA \* $P < .05$ ; \*\* $P < .001$ . Data are shown as the mean  $\pm$  SD

*aureus* infection by qRT-PCR. To further confirm our microarray data, we performed independent experiments and found *S aureus* infection induced the expression of IRE1 $\alpha$  and the splicing of *XBP1* mRNA in mice retina, indicating the onset of ER stress response (Figure 1B). However, the expression of CHOP, WSF, ER-localized DnaJ homolog 4 (ERDj4), and the disulfide isomerase PDI did not change noticeably in infected retinal tissue as compared to control (Figure 1B), indicating that ATF6 and PERK pathways are unlikely involved in *S aureus*-induced ER stress response in the retina. These observations led us to focus on the IRE1 $\alpha$ -mediated ER stress pathway in *S aureus* endophthalmitis.

To evaluate the specificity of the bacterial-induced IRE1 $\alpha$ -XBP1 axis of ER stress we used a potent pharmacological inhibitor of IRE1 $\alpha$ , 4 $\mu$ 8C, which inhibits substrate access to the active site of IRE1 leading to the inactivation of *Xbp1* splicing and IRE1-mediated mRNA degradation.<sup>38</sup> To investigate this, first, we performed a dose-response study using 4 $\mu$ 8C on mouse BV2 microglia cells<sup>10</sup> challenged with *S aureus* (Figure S1A). Because all the dosages of 4 $\mu$ 8C tested showed a reduction of *XBP1* mRNA splicing (XBP1s), we decided to use 100 nM of this inhibitor for the remainder of the study.

### 3.2 | *S aureus* induces IRE1 $\alpha$ -mediated ER stress response via TLR2

In the eye, *S aureus* has been shown to invoke retinal innate responses through TLR2 signaling<sup>4,10,11</sup> and TLRs have

been implicated in triggering ER stress,<sup>26,27</sup> we sought to decipher the link between TLR2 and IRE1 $\alpha$  activation in our disease model, which is currently unknown. To establish the role of TLR2 signaling in regulating IRE1 $\alpha$ -mediated ER stress response, *S aureus* endophthalmitis was induced in WT C57BL/6, TLR2<sup>-/-</sup>, and MyD88<sup>-/-</sup> mice with or without 4 $\mu$ 8C pretreatment. Our data shows *S aureus* infection-induced activation of IRE1 $\alpha$  and prominent splicing of *Xbp1* transcripts in WT and MyD88<sup>-/-</sup> mice and the response was attenuated by 4 $\mu$ 8C treatment. In contrast, infected TLR2<sup>-/-</sup> mouse retina did not show the splicing of XBP1 (Figure 2A). We further confirmed the IRE1 $\alpha$  activation at protein levels in retinal tissue of *S aureus* infected WT, TLR2<sup>-/-</sup>, and MyD88<sup>-/-</sup> mice by western blotting. Our results show that *S aureus* significantly induced the phosphorylation of IRE1 $\alpha$  in WT and MyD88<sup>-/-</sup> mice, whereas, its levels were significantly lower in TLR2<sup>-/-</sup> mice (Figure 2B). These results indicate that TLR2 mediates IRE1 $\alpha$ -mediated ER stress response in *S aureus* endophthalmitis.

For in vitro studies, we used mouse BV2 microglia which have been shown to respond to *S aureus* challenge analogous to that of primary retinal microglia.<sup>10</sup> To examine the role of TLRs in IRE1 $\alpha$  activation in our model, BV2 microglia were challenged with the TLR2 agonist, Pam3CSK4, and the TLR4 agonist, LPS, in the presence and absence of IRE1 $\alpha$  inhibitor 4 $\mu$ 8C; live *S aureus* (SA) was used as a positive control. Our results show all agents (Pam3CSK4, LPS, and SA) induced the expression of IRE1 $\alpha$  as well as the splicing of *XBP1* and that this response was reduced by 4 $\mu$ 8C

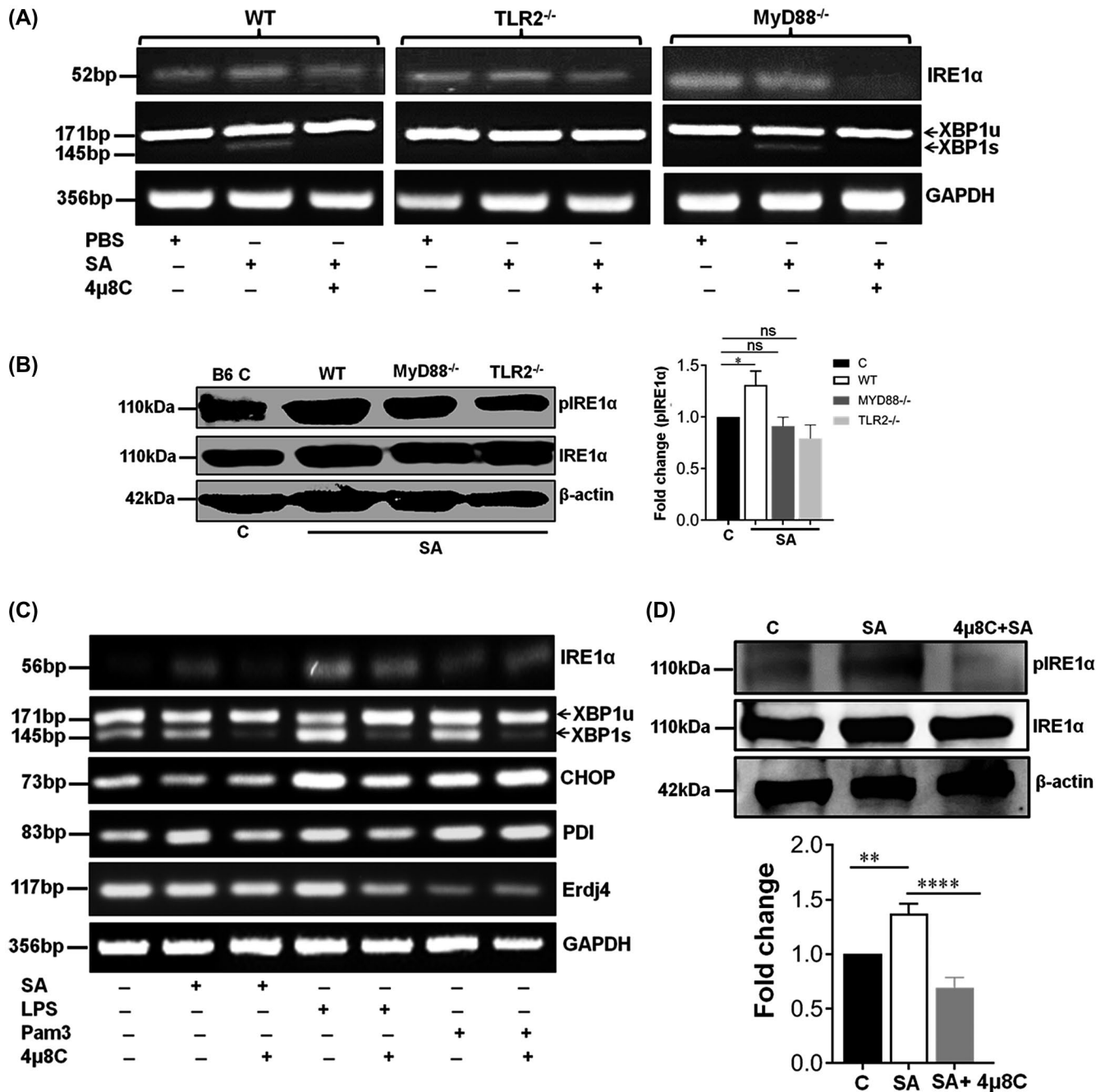


**FIGURE 2** *S aureus* induces IRE1 $\alpha$ -mediated ER stress via TLR2. C57BL/6 (WT), TLR2<sup>-/-</sup>, and MyD88<sup>-/-</sup> mouse (n = 6 each) (all on B6 background) eyes were intravitreally injected with 4 $\mu$ 8C (0.1  $\mu$ g/eye), 12 hours post drug injection, SA endophthalmitis was induced, and retinal tissue (24 hours post-SA infection) was harvested and subjected to RT-PCR to detect IRE1 $\alpha$  expression and XBP1 splicing, using GAPDH as housekeeping gene (A). The protein levels of pIRE1 $\alpha$  and IRE1 $\alpha$  were assessed by western blot (B, left panel), and band intensities were quantified using ImageJ, normalized with  $\beta$ -actin, and represented as a bar graph (B, Right panel). Mouse microglial cells (BV2 cell line) were left untreated or pre-treated with IRE1 $\alpha$  inhibitor, 4 $\mu$ 8C (100 nM), followed by challenge with *S aureus* (SA), TLR2 agonist (Pam3CSK4, 10  $\mu$ g/mL), and, TLR4 agonist (LPS, 10  $\mu$ g/mL) for 8 hours. The mRNA expression of indicated ER stress markers was assessed by RT-PCR (C). The protein levels of pIRE1 $\alpha$  and IRE1 $\alpha$  were assessed by western blot (D, left panel), and band intensities were quantified using ImageJ, normalized with  $\beta$ -actin, and represented as a bar graph (D, Right panel) Results are representative of at least three independent experiments. Statistical analysis was performed using one-way ANOVA \* $P$  < .05; \*\* $P$  < .01; \*\*\*\* $P$  < .0001; ns, not significant

treatment (Figure 2C). We also examined the activation of classical ER stress response and found no marked induction of CHOP, ERDj4, and PDI expression in response to the Pam3CSK or *S aureus* challenge (Figure 2C). Induction of

IRE1 $\alpha$  and its inhibition by 4 $\mu$ 8C was confirmed at the protein level by western blotting (Figure 2D) and immunostaining (Figure S1B), which displayed reduced phosphorylation of IRE1 $\alpha$  upon 4 $\mu$ 8C treatment in BV2 microglial cells.

In addition to specific TLR ligands, we assessed the effect of *S aureus* virulence factors ( $\alpha$ -toxin, LTA, and PGN) on ER stress response and observed that they also modestly induced the expression of IRE1 $\alpha$  and XBP1 splicing (Figure S2A).

### 3.3 | IRE1 $\alpha$ regulates *S aureus* and TLR2 ligand-induced inflammatory response

TLR-mediated ER stress response has been linked to the elicitation of innate responses in various pathological conditions.<sup>27,39,40</sup> Hyperglycemia-induced ER stress has also been implicated in retinal Müller glia-derived inflammatory response in diabetic retinopathy.<sup>41</sup> To assess the functional role of IRE1 $\alpha$  activation in *Staphylococcal* endophthalmitis, we evaluated the inflammatory mediators in mice eyes and cultured BV2 microglial cells. As expected, *S aureus* induced the production of key inflammatory cytokines, IL-1 $\beta$ , TNF- $\alpha$ , and the chemokine MIP2 in retinal tissue, whereas their levels were significantly reduced in mouse eyes pre-treated with the IRE1 $\alpha$  inhibitor 4 $\mu$ 8C (Figure 3A). Similarly, pretreatment of BV2 microglia with 4 $\mu$ 8C significantly

attenuated the inflammatory mediators induced by *S aureus* and Pam3CSK4 (Figure 3B).

Next, to further verify the role of IRE1 $\alpha$  in an *S aureus*-induced inflammatory response, we used BMDM from IRE1 $\alpha^{\text{flox/flox}}$  and myeloid cell-specific IRE1 $\alpha^{-/-}$  mice. *S aureus* challenge of IRE1 $\alpha^{\text{flox/flox}}$  BMDM resulted in robust production of pro-inflammatory cytokines (IL-1 $\beta$ , TNF- $\alpha$ , and IL-6) but this was not the case in IRE1 $\alpha^{-/-}$  BMDM (Figure 3C). Collectively, these results support the hypothesis that IRE1 $\alpha$  mediates an innate inflammatory response in both *Staphylococcal* endophthalmitis and cultured immune cells (microglia and macrophages).

### 3.4 | Inhibition of IRE1 $\alpha$ attenuates *S aureus*-induced NF- $\kappa$ B and MAPK signaling

Because NF- $\kappa$ B and other MAP kinases, such as ERK and p38 are known to regulate the inflammatory response in *S aureus* endophthalmitis,<sup>10,30,42</sup> we decided to assess their link with IRE1 $\alpha$  activation.<sup>43</sup> *Staphylococcal* endophthalmitis was induced in WT mouse eyes pretreated with 4 $\mu$ 8C, and western blot was performed to detect I $\kappa$ B and MAPKs in

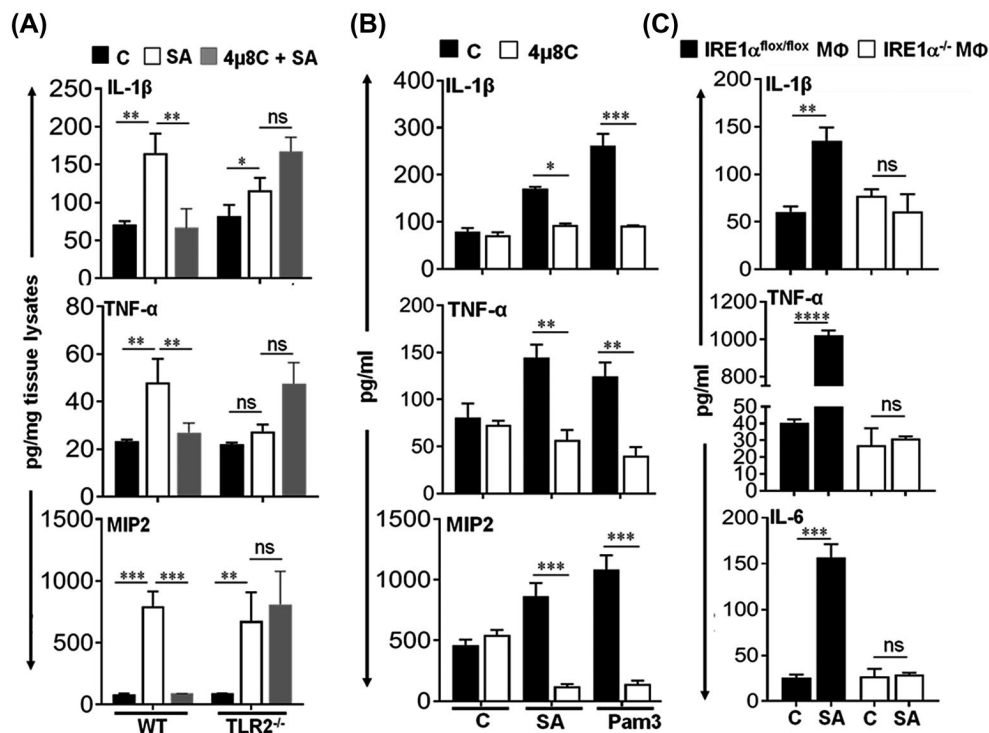


**FIGURE 3** IRE1 $\alpha$  regulates *S aureus* and TLR2 ligand-induced inflammatory response. C57BL/6 (WT) and TLR2 $^{-/-}$  mouse (n = 6 per group) eyes were injected with IRE1 $\alpha$  inhibitor, 4 $\mu$ 8C (0.1  $\mu$ g/eye), 12 hours prior to induction of *S aureus* endophthalmitis and at 24 hours postinfection eye lysates were subjected to ELISA for measurements of indicated cytokines/chemokines (A). BV2 microglial cells were pre-treated with 4 $\mu$ 8C (100 nM, for 1 hour) followed by challenge with SA (MOI 10:1), and Pam3CSK4 (10  $\mu$ g/mL) for 8 hours. The conditioned media was used for ELISA for the quantification of indicated cytokines/chemokines (B). The production of inflammatory mediators was assessed in IRE1 $\alpha^{\text{flox/flox}}$ , and myeloid cell-specific IRE1 $\alpha^{-/-}$  BMDM (M $\Phi$ ) challenged with SA (MOI 10:1) for 8 hours using ELISA (C). Results are cumulative of at least two independent (n = 6 each) experiments. Statistical analysis was performed using Student's *t* test \**P* < .05; \*\**P* < .01; \*\*\**P* < .001; \*\*\*\**P* < .0001; ns, not significant. Data are shown as the mean  $\pm$  SD

retinal tissue lysates. Our results show that *S aureus*-induced phosphorylation of I $\kappa$ B, ERK1/2, and p38 proteins, whereas, IRE1 $\alpha$  inhibition reduced the activation of these signaling molecules (Figure 4A). Similarly, the pathway-specific inhibitors for I $\kappa$ B, ERK1/2, and p38 reduced *S aureus*-induced *Xbp1* splicing (Figure 4B), indicating the existence of a feedback inhibition system among these pathways. The activity of these pathway inhibitors was validated by assessing *S aureus*-induced mRNA expression of the inflammatory cytokine *Il-1 $\beta$*  (Figure S2B). Together, these results suggest that IRE1 $\alpha$  is an upstream regulator of *S aureus*-induced NF- $\kappa$ B and MAPKs signaling.

### 3.5 | *S aureus*-induced ROS activates IRE1 $\alpha$ -XBP-mediated ER stress response

A correlation between ROS generation and the induction of ER stress has been shown in several pathological conditions.<sup>44-46</sup> Previously, we have shown that *S aureus* induces ROS generation in retinal cells.<sup>9</sup> Therefore, we sought to investigate whether *S aureus*-induced ROS production plays any role in the IRE1 $\alpha$ -mediated ER stress response. To

investigate this, we used Diphenyleneiodonium (DPI), an NAD(P)H oxidase inhibitor, and a potent ROS blocker. Our data showed DPI pretreatment in BV2 microglia, reduced *S aureus*-triggered IRE1 $\alpha$  expression as well as *Xbp1* splicing (Figure 5A). Moreover, the conditioned media from DPI-treated cells showed reduced accumulation of inflammatory mediators (Figure 5B). This observation indicates that *S aureus*-induced ROS generation contributes to the induction of ER stress, and blocking ROS production could prevent *S aureus*-induced ER stress.

### 3.6 | IRE1 $\alpha$ inhibition results in increased bacterial burden and tissue damage in the eye

ER stress can either promote or impede disease progression depending on the disease model, cell types, and the ER stress sensors involved.<sup>47-49</sup> Studies have shown that some intracellular pathogens use ER stress signaling as a protective mechanism for their intracellular growth, making IRE1 $\alpha$ -induced UPR beneficial for the spread of infection.<sup>25,50,51</sup> Since found that *S aureus*-induced IRE1 $\alpha$  activation and *Xbp1* splicing both in vivo and in vitro, and IRE1 $\alpha$  inhibition diminished

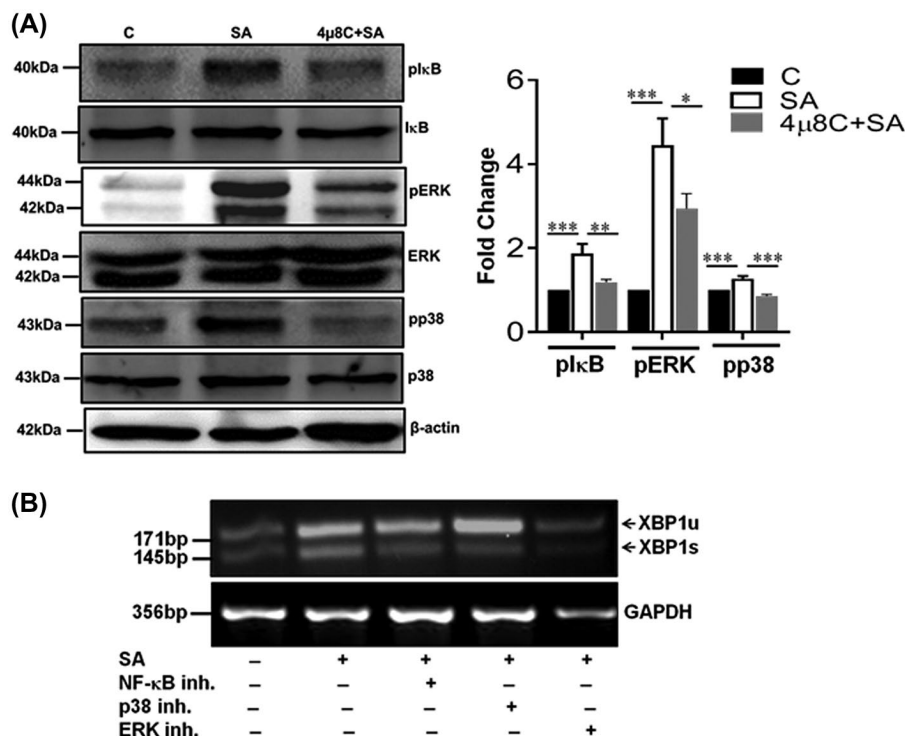


**FIGURE 4** IRE1 $\alpha$  inhibition attenuates *S aureus*-induced NF- $\kappa$ B and MAPK signaling. C57BL/6 mouse ( $n = 6$  per group) eyes were injected with IRE1 $\alpha$  inhibitor, 4 $\mu$ 8C (0.1  $\mu$ g/eye), 12 hours prior to the induction of *S aureus* (SA) endophthalmitis. At 24 hours postinfection, retinal tissue lysates were subjected to western blot analysis for pI $\kappa$ B, pERK, and pp38 signaling pathways (A, Left panel). Band intensities were quantified using ImageJ, normalized with  $\beta$ -actin, and represented as fold change in a bar graph (A, Right panel). BV2 cells were pre-treated for 1 hour with NF- $\kappa$ B, p38, and ERK inhibitors (10  $\mu$ M each) followed by SA (MOI 10:1) challenge for 8 hours. Total RNA was extracted, reverse transcribed, and subjected to RT-PCR for XBP1 spliced (XBP1s) and unspliced (XBP1u) forms. Statistical analysis was performed using one-way ANOVA. Data represent mean  $\pm$  SD. from two independent ( $n = 6$  each) experiments \* $P < .05$ ; \*\* $P < .01$ ; \*\*\* $P < .001$



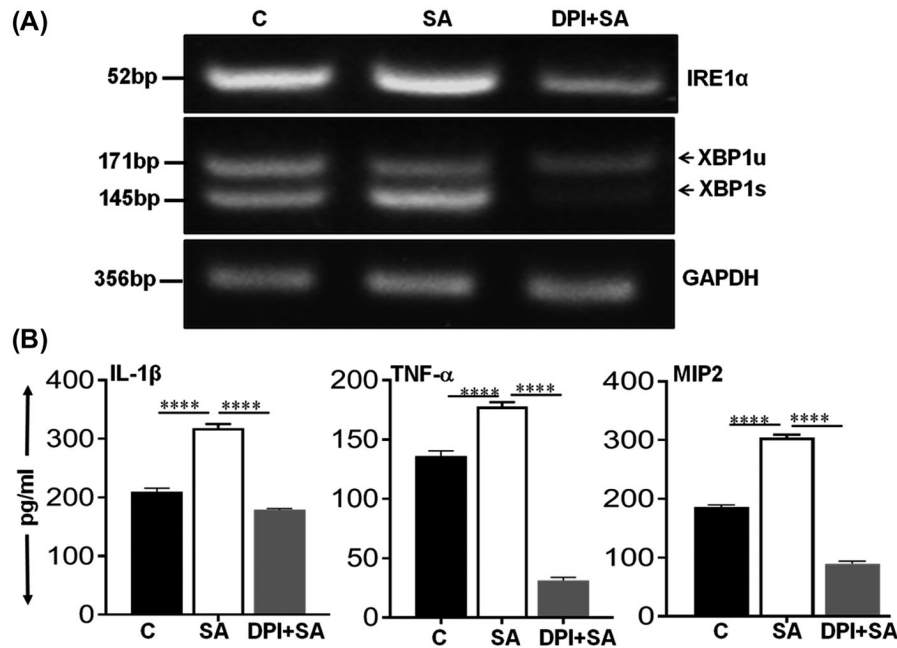


**FIGURE 5** ROS inhibition reduces *S aureus*-induced XBP1 splicing and inflammatory mediators. BV2 microglial cells were left untreated or pre-treated with NADPH oxidase inhibitor, DPI (1  $\mu$ M) for 1 hour followed by *S aureus* (SA) challenge for 8 hours. Total RNA was extracted, reverse transcribed, and subjected to RT-PCR for detection of IRE1 $\alpha$  and XBP1 (unspliced: XBPu, spliced: XBP1s) (A). ELISA was performed from conditioned media for indicated cytokines/chemokines quantification (B). Results are cumulative of at least three independent experiments. Statistical analysis was performed using Student's *t* test, \*\*\*\**P* < .0001. Data are shown as the mean  $\pm$  SD

pro-inflammatory cytokine production, we sought to determine the effect of IRE1 $\alpha$  inhibition (4 $\mu$ 8C treatment) on disease progression. First, we assessed the intraocular bacterial burden, and unexpectedly, we found that IRE1 $\alpha$  inhibition resulted in higher bacterial load in the eyes as compared to *S aureus* alone injected eyes. (Figure 6A). To assess *S aureus*-induced disease pathology, we performed histological analysis and our data showed increased retinal damage (retinal folding and disintegration of retinal layers), and fibrin formation in 4 $\mu$ 8C-treated eyes compared to eyes only infected with *S aureus* (Figure 6B). This observation was confirmed by TUNEL staining of retinal sections which showed more TUNEL positive cells in eyes treated with the IRE1 $\alpha$  inhibitor, 4 $\mu$ 8C (Figure 5C), indicating increased retinal cell death. We also performed flow cytometry to assess PMN infiltration and found significantly reduced PMN infiltration in the retina upon IRE1 $\alpha$  inhibition (Figure 6D). Altogether, these results indicate that IRE1 $\alpha$ -mediated ER stress is essential in controlling disease pathology in bacterial endophthalmitis.

## 4 | DISCUSSION

This study demonstrates that IRE1 $\alpha$ /XBP1 axis of ER stress pathways plays a pivotal role in the eye during bacterial (*S aureus*) endophthalmitis through regulation of innate inflammatory responses. The pharmacological inhibition of this pathway markedly increased disease severity by increasing

bacterial proliferation and more retinal tissue damage in the eye. Most importantly, we found that bacterial-induced IRE1 $\alpha$ /XBP1 signaling was TLR2 dependent. Since the attenuation of ER stress has been mostly shown beneficial in eye diseases,<sup>52-54</sup> our study reveals what we believe an unconventional role for the IRE1 $\alpha$ /XBP1 pathway as a crucial regulator of ocular innate immunity (Figure 7).

Our rationale of the current study emerged from an earlier transcriptomics analysis,<sup>29</sup> showing induced expression of *Xbp1* and *Bip* transcripts in *S aureus* infected mouse retina, indicating their role in the pathobiology of bacterial endophthalmitis. Although, several ER stress pathways can be triggered in mammalian cells under infectious and inflammatory conditions, we did not observe the activation of ATF6 or the PERK pathway. We, therefore, hypothesized that the primary pathway involved in our disease model is the IRE1 $\alpha$ -XBP1 pathway. This is supported by multiple pieces of evidence, including, splicing of IRE1 $\alpha$  downstream target XBP1 and the attenuation of an inflammatory response and severe disease pathology by pharmacological inhibition of IRE1 $\alpha$ . These observations corroborate with studies where activation of IRE1-XBP1-mediated ER stress has also been reported via various intracellular pathogens such as *Chlamydia trachomatis*,<sup>55</sup> *Brucella abortus*,<sup>56</sup> and *Francisella tularensis*.<sup>27</sup> However, some other bacterial species and their toxins such as subtilase toxin produced by *Escherichia coli*,<sup>57</sup> and listeriolysin O, produced by *Listeria monocytogenes*<sup>58</sup> have been shown to activate other arms of the UPR as well. In addition to live

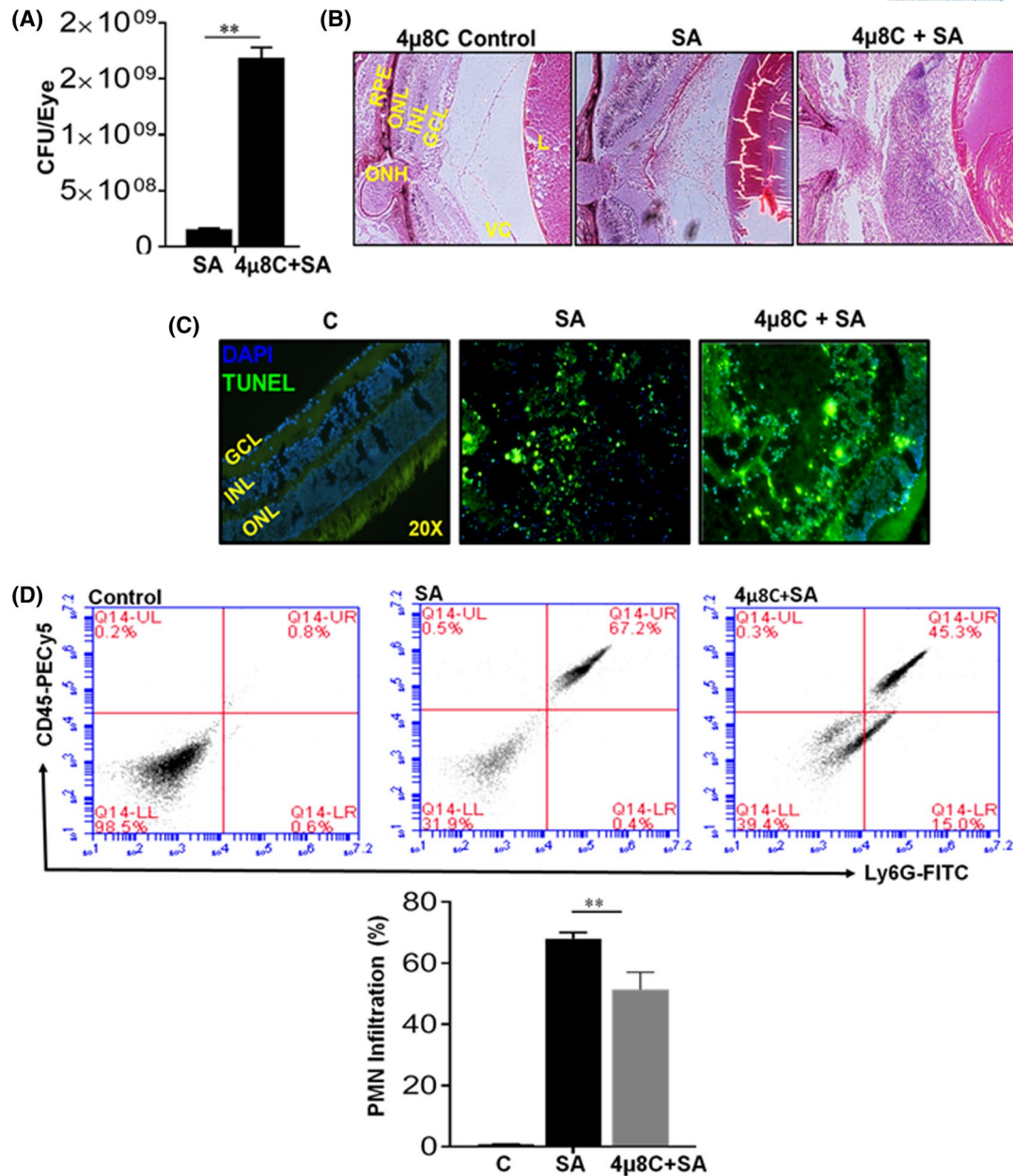


**FIGURE 6** IRE1 $\alpha$  inhibition aggravates disease pathology in mouse eyes. Eyes of C57BL/6 WT mouse ( $n = 6$ ) were pre-treated by intravitreal injection with 4 $\mu$ 8C (0.1  $\mu$ g/eye), followed by induction of *S aureus* (SA) endophthalmitis. Twenty-four hours post-SA infection, eyes were enucleated, lysate was prepared in sterile PBS, and the bacterial count was measured by serial plate dilution and represented as CFU per eye (A). Histological analysis was performed at 24 hours postinfection by paraffin embedding and H&E staining. 4 $\mu$ 8C alone injected eyes were used as control (B). Retinal cell death was visualized by TUNEL staining on cryosections showing TUNEL-positive cells (green) and DAPI stained nuclei (blue) (C). Flow cytometry was used to assess PMN infiltration by pooling retina from two eyes and staining single-cell suspensions with anti-CD45-PECy5 and anti-Ly6G-FITC monoclonal antibodies (D). Representative dot plots show the percentage of dually positive PMNs (upper right quadrants in upper panel). The bar graph shows cumulative quantitative data from three independent experiments (lower panel). (GCL, ganglion cell layer; INL, inner nuclear layer; L, lens; ONH, optic nerve head; ONL, outer nuclear layer; RPE, retinal pigmented epithelium layer; VC, vitreous chamber) Statistical analysis was performed using Student's *t* test. Data represent mean  $\pm$  SD from two independent ( $n = 6$  each) experiments  $**P < .01$

*S aureus* infection, we found that TLR2 ligand, Pam3CSK4, and other *S aureus* virulence factors (PGN, LTA, and  $\alpha$ -toxin) also activate the IRE1-XBP1 pathway, indicating the potential involvement of TLR2 signaling in regulating an IRE1-mediated ER stress response. Moreover, LPS-induced IRE1 $\alpha$

activation through TRAF6 has also been reported by Zhang and co-workers in collaboration with our laboratory.<sup>59</sup> Consistent with our data, other studies have suggested that TLR2 can activate the IRE1 $\alpha$  pathway, but not the ATF6 or PERK pathways.<sup>27</sup>

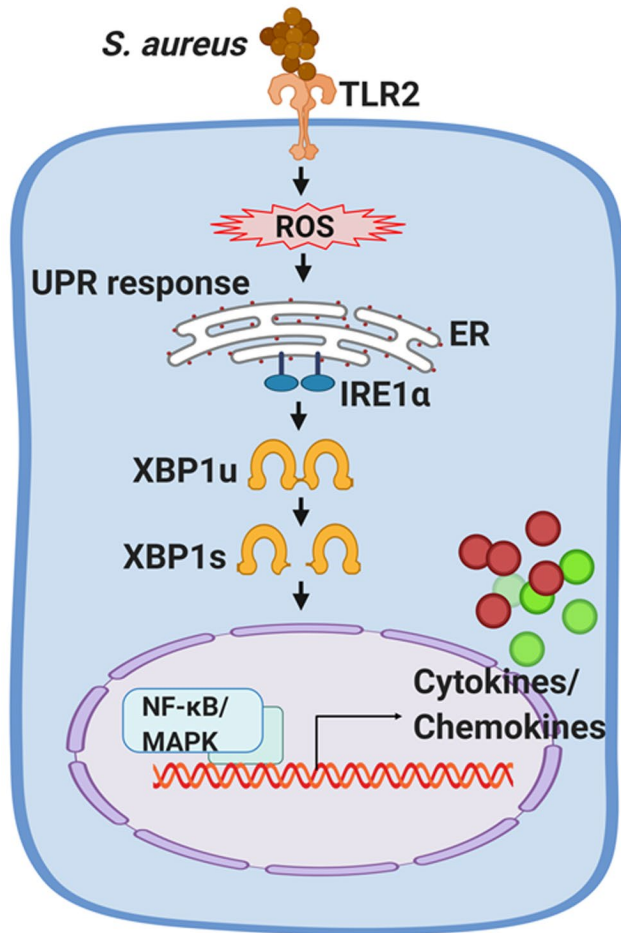


**FIGURE 7** A schematic illustration of IRE1 $\alpha$  in regulating the innate inflammatory response in bacterial endophthalmitis. TLR2 recognizes *S. aureus* and induces IRE1 $\alpha$  activation through ROS generation. This causes splicing of IRE1 $\alpha$  downstream target, XBP1, which activates NF- $\kappa$ B and MAPK signaling resulting in the production of pro-inflammatory cytokines/chemokines. *S. aureus* infection primarily induces, IRE1 $\alpha$ -XBP1 axis of the ER stress response. The schematic diagram was created using BioRender software

Furthermore, we established the role of TLR2 signaling in *S. aureus*-induced ER stress using TLR2 and its downstream adaptor, MyD88 deficient mice. We found that *S. aureus*-induced IRE1 $\alpha$ -mediated ER stress is TLR2 dependent but only partially dependent on MyD88 pathways. Prior reports have shown impaired XBP1 splicing in TLR2-deficient macrophages following TLR2 agonists Pam3CSK4, FSL1, *F. tularensis* challenge, and MRSA infection.<sup>27,45</sup> Similarly, *Xbp1* splicing has been reported in macrophages by both MyD88 dependent and independent mechanisms.<sup>27</sup> Both TLR-signaling and IRE1-mediated splicing of *Xbp1* have been shown to invoke innate immune responses and the production of inflammatory cytokines.<sup>27,36,45,60</sup> Our data demonstrated that inhibiting IRE1 $\alpha$  attenuates *S. aureus*-induced cytokine production in vivo (mouse model of endophthalmitis) as well

as in cultured microglia, implicating its role in regulating the inflammatory innate immune response. The experiments using BMDM from myeloid cell-specific IRE1 $^{-/-}$  mice further validates these findings by showing inhibition of *S. aureus*-induced inflammatory mediators. Thus, we conclude that TLR2 triggers IRE1 $\alpha$  activation to initiate an innate immune response in *S. aureus* endophthalmitis.

Previous studies from our laboratory and other investigators have shown that in ocular infections, NF- $\kappa$ B and MAPK activation are key players in orchestrating inflammatory responses by various retinal cell types.<sup>10,30,42</sup> In this study, we demonstrated that in response to *S. aureus* infection, IRE1 $\alpha$ -mediated ER stress controls the activation of NF- $\kappa$ B, and MAPK such as ERK, and p38 signaling pathways. Similarly, the inhibition of these pro-inflammatory signaling pathways using their pharmacological inhibitors, resulted in impaired splicing of *Xbp1*, suggesting positive feedback inhibition of ER stress. These results indicate that diminished pro-inflammatory cytokines production upon IRE1 inhibition could be due to the downregulation of *S. aureus*-induced NF- $\kappa$ B and MAPK activation.

Reactive oxygen species (ROS) production and ER stress induction are a part of a positive feedback loop.<sup>47,61</sup> Innate immune cells also utilize ROS to kill pathogens, including *S. aureus*.<sup>9,45</sup> We previously showed *S. aureus* infection lead to ROS production in retinal cells.<sup>9</sup> Our experiment utilizing NADPH oxidase inhibitor, DPI, resulted in reduced *Xbp1* splicing and diminished production of inflammatory cytokine, establishes a link between ROS generation and IRE1 $\alpha$  activation.<sup>45</sup> Our data showed an increased bacterial burden in the eyes upon IRE1 $\alpha$  inhibition, indicating that IRE1 $\alpha$ -mediated ER stress contributes toward antibacterial activity. Since we observed reduced PMN infiltration in eyes treated with IRE1 $\alpha$  inhibitor, it remains to be elucidated whether the increased bacterial burden is due to reduced ROS generation within PMNs, less PMN recruitment, or a combination of both and warrants further investigation. IRE1 $\alpha$  deficiency has been shown to reduce bacterial killing both in vivo as well as in vitro models<sup>47</sup> resulting in extensive liver damage in *F. tularensis* infection.<sup>27</sup> These observations coincide with our findings of elevated bacterial burden with increased retinal tissue damage due to IRE1 $\alpha$  inhibition.

In summary, our study demonstrates an essential role of IRE1 $\alpha$ -mediated ER stress response in orchestrating the retinal innate immune responses in bacterial endophthalmitis. We also found that an IRE1 $\alpha$ -mediated innate immune response is regulated by TLR2, which has been shown to exert a protective effect in *S. aureus* endophthalmitis. These findings uncover an important mechanism that can modulate ocular inflammation and could, therefore, provide new opportunities for the development of anti-inflammatory therapies and treatments for ocular infections.

## ACKNOWLEDGMENTS

This study was supported by NIH grants R01EY026964, R01EY027381, R21AI140033, and R21AI135583 (to AK). Our research is also supported in part by an unrestricted grant to the Kresge Eye Institute/Department of Ophthalmology, Visual, and Anatomical Sciences from Research to Prevent Blindness Inc. The study was partially supported by NIH grant DK090313 (to KZ). The immunology resource core is supported by an NIH center grant P30EY004068. The authors thank Robert Wright for critical editing of the final manuscript. The funders had no role in study design, data collection, and interpretation, or the decision to submit the work for publication.

## CONFLICT OF INTEREST

The authors declare no conflict of interest.

## AUTHOR CONTRIBUTIONS

Ajay Kumar, Pawan K. Singh, and Ashok Kumar conceived the project and designed the experiments; Ajay Kumar and Pawan K. Singh performed the experiments and analyzed the data; K. Zhang and Ashok Kumar contributed reagents/materials/analysis tools; Ajay Kumar, Pawan K. Singh, and Ashok Kumar wrote the manuscript. All authors reviewed and approved the final version of the manuscript.

## REFERENCES

- Lowy FD. Staphylococcus aureus infections. *N Engl J Med.* 1998;339:520-532.
- Musher DM, Lamm N, Darouiche RO, Young EJ, Hamill RJ, Landon GC. The current spectrum of *Staphylococcus aureus* infection in a tertiary care hospital. *Medicine (Baltimore).* 1994;73:186-208.
- Boucher H, Miller LG, Razonable RR. Serious infections caused by methicillin-resistant *Staphylococcus aureus*. *Clin Infect Dis.* 2010;51(Suppl. 2):S183-S197.
- Talreja D, Singh PK, Kumar A. In vivo role of TLR2 and MyD88 signaling in eliciting innate immune responses in staphylococcal endophthalmitis. *Invest Ophthalmol Vis Sci.* 2015;56:1719-1732.
- Miller FC, Coburn PS, Huzzatul MM, LaGrow AL, Livingston E, Callegan MC. Targets of immunomodulation in bacterial endophthalmitis. *Prog Retin Eye Res.* 2019;73:100763.
- Miller JJ, Scott IU, Flynn HW Jr, Smiddy WE, Newton J, Miller D. Acute-onset endophthalmitis after cataract surgery (2000-2004): incidence, clinical settings, and visual acuity outcomes after treatment. *Am J Ophthalmol.* 2005;139:983-987.
- Hanscom T. The Endophthalmitis vitrectomy study. *Arch Ophthalmol.* 1996;114:1029-1030; author reply 1028-1029.
- Singh PK, Kumar A. Retinal photoreceptor expresses toll-like receptors (TLRs) and elicits innate responses following TLR ligand and bacterial challenge. *PLoS One.* 2015;10:e0119541.
- Singh PK, Shiha MJ, Kumar A. Antibacterial responses of retinal Muller glia: production of antimicrobial peptides, oxidative burst and phagocytosis. *J Neuroinflammation.* 2014;11:33.
- Kochan T, Singla A, Tosi J, Kumar A. Toll-like receptor 2 ligand pretreatment attenuates retinal microglial inflammatory response but enhances phagocytic activity toward *Staphylococcus aureus*. *Infect Immun.* 2012;80:2076-2088.
- Kumar A, Singh CN, Glybina IV, Mahmoud TH, Yu FS. Toll-like receptor 2 ligand-induced protection against bacterial endophthalmitis. *J Infect Dis.* 2010;201:255-263.
- Coburn PS, Miller FC, LaGrow AL, et al. TLR4 modulates inflammatory gene targets in the retina during *Bacillus cereus* endophthalmitis. *BMC Ophthalmol.* 2018;18:96.
- Parkunan SM, Randall CB, Coburn PS, Astley RA, Staats RL, Callegan MC. Unexpected roles for toll-like receptor 4 and TRIF in intraocular infection with gram-positive bacteria. *Infect Immun.* 2015;83:3926-3936.
- Chang JH, McCluskey PJ, Wakefield D. Toll-like receptors in ocular immunity and the immunopathogenesis of inflammatory eye disease. *Br J Ophthalmol.* 2006;90:103-108.
- Pandey RK, Yu FS, Kumar A. Targeting toll-like receptor signaling as a novel approach to prevent ocular infectious diseases. *Indian J Med Res.* 2013;138:609-619.
- Lin JH, Walter P, Yen TS. Endoplasmic reticulum stress in disease pathogenesis. *Annu Rev Pathol.* 2008;3:399-425.
- Xu C, Bailly-Maitre B, Reed JC. Endoplasmic reticulum stress: cell life and death decisions. *J Clin Invest.* 2005;115:2656-2664.
- Yoshida H, Matsui T, Yamamoto A, Okada T, Mori K. XBP1 mRNA is induced by ATF6 and spliced by IRE1 in response to ER stress to produce a highly active transcription factor. *Cell.* 2001;107:881-891.
- Newton PM, Ron D. Protein kinase C and alcohol addiction. *Pharmacol Res.* 2007;55:570-577.
- Zhang K, Wang S, Malhotra J, et al. The unfolded protein response transducer IRE1alpha prevents ER stress-induced hepatic steatosis. *EMBO J.* 2011;30:1357-1375.
- Kanemoto S, Kondo S, Ogata M, Murakami T, Urano F, Imaizumi K. XBP1 activates the transcription of its target genes via an ACGT core sequence under ER stress. *Biochem Biophys Res Commun.* 2005;331:1146-1153.
- Schroder M, Kaufman RJ. The mammalian unfolded protein response. *Annu Rev Biochem.* 2005;74:739-789.
- Nau GJ, Richmond JF, Schlesinger A, Jennings EG, Lander ES, Young RA. Human macrophage activation programs induced by bacterial pathogens. *Proc Natl Acad Sci U S A.* 2002;99:1503-1508.
- Blumenthal A, Lauber J, Hoffmann R, et al. Common and unique gene expression signatures of human macrophages in response to four strains of *Mycobacterium avium* that differ in their growth and persistence characteristics. *Infect Immun.* 2005;73:3330-3341.
- Celli J, Tsohis RM. Bacteria, the endoplasmic reticulum and the unfolded protein response: friends or foes? *Nat Rev Microbiol.* 2015;13:71-82.
- Choi JA, Song CH. Insights into the role of endoplasmic reticulum stress in infectious diseases. *Front Immunol.* 2019;10:3147.
- Martinon F, Chen X, Lee AH, Glimcher LH. TLR activation of the transcription factor XBP1 regulates innate immune responses in macrophages. *Nat Immunol.* 2010;11:411-418.
- Qiu Q, Zheng Z, Chang L, et al. Toll-like receptor-mediated IRE1alpha activation as a therapeutic target for inflammatory arthritis. *EMBO J.* 2013;32:2477-2490.
- Rajamani D, Singh PK, Rottmann BG, Singh N, Bhasin MK, Kumar A. Temporal retinal transcriptome and systems biology analysis identifies key pathways and hub genes in *Staphylococcus aureus* endophthalmitis. *Sci Rep.* 2016;6:21502.
- Kumar A, Giri S, Kumar A. 5-Aminoimidazole-4-carboxamide ribonucleoside-mediated adenosine monophosphate-activated protein kinase activation induces protective innate responses in bacterial endophthalmitis. *Cell Microbiol.* 2016;18:1815-1830.

31. Swamydas M, Lionakis MS. Isolation, purification and labeling of mouse bone marrow neutrophils for functional studies and adoptive transfer experiments. *J Vis Exp*. 2013;77:e50586.
32. Singh PK, Donovan DM, Kumar A. Intravitreal injection of the chimeric phage endolysin Ply187 protects mice from *Staphylococcus aureus* endophthalmitis. *Antimicrob Agents Chemother*. 2014;58:4621-4629.
33. Singh S, Singh PK, Suhail H, et al. AMP-activated protein kinase restricts zika virus replication in endothelial cells by potentiating innate antiviral responses and inhibiting glycolysis. *J Immunol*. 2020;204:1810-1824.
34. Singh PK, Guest J-M, Kanwar M, et al. Zika virus infects cells lining the blood-retinal barrier and causes chorioretinal atrophy in mouse eyes. *JCI Insight*. 2017;2:e92340.
35. Roybal CN, Yang S, Sun CW, et al. Homocysteine increases the expression of vascular endothelial growth factor by a mechanism involving endoplasmic reticulum stress and transcription factor ATF4. *J Biol Chem*. 2004;279:14844-14852.
36. Pillich H, Loose M, Zimmer KP, Chakraborty T. Diverse roles of endoplasmic reticulum stress sensors in bacterial infection. *Mol Cell Pediatr*. 2016;3:9.
37. Calfon M, Zeng H, Urano F, et al. IRE1 couples endoplasmic reticulum load to secretory capacity by processing the XBP-1 mRNA. *Nature*. 2002;415:92-96.
38. Cross BCS, Bond PJ, Sadowski PG, et al. The molecular basis for selective inhibition of unconventional mRNA splicing by an IRE1-binding small molecule. *Proc Natl Acad Sci U S A*. 2012;109:E869-E878.
39. Liao K, Guo M, Niu F, Yang L, Callen SE, Buch S. Cocaine-mediated induction of microglial activation involves the ER stress-TLR2 axis. *J Neuroinflammation*. 2016;13:33.
40. Coope A, Milanski M, Arruda AP, et al. Chaperone insufficiency links TLR4 protein signaling to endoplasmic reticulum stress. *J Biol Chem*. 2012;287:15580-15589.
41. Zhong Y, Li J, Chen Y, Wang JJ, Ratan R, Zhang SX. Activation of endoplasmic reticulum stress by hyperglycemia is essential for Muller cell-derived inflammatory cytokine production in diabetes. *Diabetes*. 2012;61:492-504.
42. Kumar A, Yin J, Zhang J, Yu FS. Modulation of corneal epithelial innate immune response to pseudomonas infection by flagellin pretreatment. *Invest Ophthalmol Vis Sci*. 2007;48:4664-4670.
43. Kim HT, Qiang W, Liu N, Scofield VL, Wong PK, Stoica G. Up-regulation of astrocyte cyclooxygenase-2, CCAAT/enhancer-binding protein-homology protein, glucose-related protein 78, eukaryotic initiation factor 2 alpha, and c-Jun N-terminal kinase by a neurovirulent murine retrovirus. *J Neurovirol*. 2005;11:166-179.
44. Cao SS, Kaufman RJ. Endoplasmic reticulum stress and oxidative stress in cell fate decision and human disease. *Antioxid Redox Signal*. 2014;21:396-413.
45. Abuaita BH, Burkholder KM, Boles BR, O'Riordan MX. The endoplasmic reticulum stress sensor inositol-requiring enzyme 1alpha augments bacterial killing through sustained oxidant production. *mBio*. 2015;6:e00705.
46. Ozgur R, Uzilday B, Iwata Y, Koizumi N, Turkan I. Interplay between the unfolded protein response and reactive oxygen species: a dynamic duo. *J Exp Bot*. 2018;69:3333-3345.
47. Senft D, Ronai ZA. UPR, autophagy, and mitochondria cross-talk underlies the ER stress response. *Trends Biochem Sci*. 2015;40:141-148.
48. Chen S, Zhang D. Friend or foe: endoplasmic reticulum protein 29 (ERp29) in epithelial cancer. *FEBS Open Bio*. 2015;5:91-98.
49. Cunard R. Endoplasmic reticulum stress in the diabetic kidney, the good, the bad and the ugly. *J Clin Med*. 2015;4:715-740.
50. Smith JA, Khan M, Magnani DD, et al. Brucella induces an unfolded protein response via TcpB that supports intracellular replication in macrophages. *PLoS Pathog*. 2013;9:e1003785.
51. Qin QM, Pei J, Ancona V, Shaw BD, Ficht TA, de Figueiredo P. RNAi screen of endoplasmic reticulum-associated host factors reveals a role for IRE1alpha in supporting Brucella replication. *PLoS Pathog*. 2008;4:e1000110.
52. Kroeger H, Chiang WC, Felden J, Nguyen A, Lin JH. ER stress and unfolded protein response in ocular health and disease. *FEBS J*. 2019;286:399-412.
53. Zode GS, Sharma AB, Lin X, et al. Ocular-specific ER stress reduction rescues glaucoma in murine glucocorticoid-induced glaucoma. *J Clin Investig*. 2014;124:1956-1965.
54. Bhatta M, Chatpar K, Hu Z, Wang JJ, Zhang SX. Reduction of endoplasmic reticulum stress improves angiogenic progenitor cell function in a mouse model of type 1 diabetes. *Cell Death Dis*. 2018;9:467.
55. Webster SJ, Ellis L, O'Brien LM, et al. IRE1alpha mediates PKR activation in response to *Chlamydia trachomatis* infection. *Microbes Infect*. 2016;18:472-483.
56. de Jong MF, Starr T, Winter MG, et al. Sensing of bacterial type IV secretion via the unfolded protein response. *mBio*. 2013;4:e00418-12.
57. Morinaga N, Yahiro K, Matsuura G, Moss J, Noda M. Subtilase cytotoxin, produced by Shiga-toxicogenic *Escherichia coli*, transiently inhibits protein synthesis of Vero cells via degradation of BiP and induces cell cycle arrest at G1 by downregulation of cyclin D1. *Cell Microbiol*. 2008;10:921-929.
58. Pillich H, Loose M, Zimmer KP, Chakraborty T. Activation of the unfolded protein response by *Listeria monocytogenes*. *Cell Microbiol*. 2012;14:949-964.
59. Dandekar A, Qiu Y, Kim H, et al. Toll-like receptor (TLR) signaling interacts with CREBH to modulate high-density lipoprotein (HDL) in response to bacterial endotoxin. *J Biol Chem*. 2016;291:23149-23158.
60. Osowski CM, Hara T, O'Sullivan-Murphy B, et al. Thioredoxin-interacting protein mediates ER stress-induced beta cell death through initiation of the inflammasome. *Cell Metab*. 2012;16:265-273.
61. Chong WC, Shastri MD, Eri R. Endoplasmic reticulum stress and oxidative stress: a vicious nexus implicated in bowel disease pathophysiology. *Int J Mol Sci*. 2017;18:771.

## SUPPORTING INFORMATION

Additional supporting information may be found online in the Supporting Information section.

**How to cite this article:** Kumar A, Singh PK, Zhang K, Kumar A. Toll-like receptor 2 (TLR2) engages endoplasmic reticulum stress sensor IRE1 $\alpha$  to regulate retinal innate responses in *Staphylococcus aureus* endophthalmitis. *The FASEB Journal*. 2020;34:13826–13838. <https://doi.org/10.1096/fj.202001393R>